

# The mid-infrared spectroscopy: A novel non-invasive diagnostic tool for NASH diagnosis in severe obesity

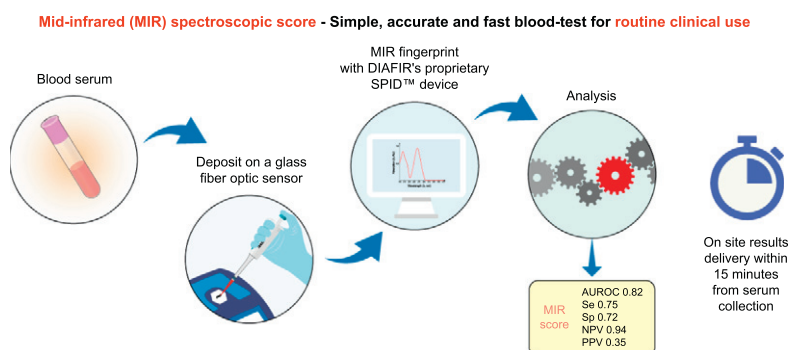
## Authors

Rodolphe Anty, Marie Morvan, Maëna Le Corvec, Clémence M Canivet, Stéphanie Patouraux, Jean Gugenheim, Stéphanie Bonnafous, Béatrice Bailly-Maitre, Olivier Sire, Hugues Tariel, Jérôme Bernard, Thierry Piche, Olivier Loréal, Judith Aron-Wisnewsky, Karine Clément, Albert Tran, Antonio Iannelli, Philippe Gual

## Correspondence

anty.r@chu-nice.fr (R. Anty)

## Graphical abstract



## Highlights

- There is no validated non-invasive diagnostic tool for NASH in routine care.
- NASH follow-up requires a non-invasive diagnostic method.
- Using a simple drop of serum, the mid-infrared spectrum captures a patient's metabolic fingerprint.
- A model based on mid-infrared spectroscopy provides efficient NASH screening for patients with severe obesity.

## Lay summary

There is an urgent need for tools to non-invasively diagnose and monitor non-alcoholic steatohepatitis (NASH). This study evaluates the performance of a new tool for fast NASH diagnosis based on mid-infrared (MIR) spectroscopy. Using serum samples from severely obese patients who underwent a bariatric procedure, which enabled a concomitant liver biopsy to be performed, the MIR spectroscopy model performed well in screening patients for NASH compared to a traditional, histological diagnosis.

<https://doi.org/10.1016/j.jhepr.2019.09.005>



# The mid-infrared spectroscopy: A novel non-invasive diagnostic tool for NASH diagnosis in severe obesity

Rodolphe Anty,<sup>1,†,\*</sup> Marie Morvan,<sup>2,†</sup> Maëna Le Corvec,<sup>3</sup> Clémence M Canivet,<sup>1</sup> Stéphanie Patouraux,<sup>1</sup> Jean Gugenheim,<sup>1</sup> Stéphanie Bonnafous,<sup>1</sup> Béatrice Bailly-Maitre,<sup>4</sup> Olivier Sire,<sup>5</sup> Hugues Tariel,<sup>3</sup> Jérôme Bernard,<sup>3</sup> Thierry Piche,<sup>1</sup> Olivier Loréal,<sup>6</sup> Judith Aron-Wisniewsky,<sup>7</sup> Karine Clément,<sup>7</sup> Albert Tran,<sup>1</sup> Antonio Iannelli,<sup>1</sup> Philippe Gual<sup>1</sup>

<sup>1</sup>Université Côte d'Azur, CHU, INSERM, U1065, C3M, France; <sup>2</sup>University of Rennes, CNRS, IRMAR - UMR, 6625, Rennes, France; <sup>3</sup>DIAFIR, Avenue Chardonnet, Parc Lorans 26 J, Rennes; <sup>4</sup>Université Côte d'Azur, INSERM, U1065, C3M, France; <sup>5</sup>IRDL UMR CNRS 6027, Vannes; <sup>6</sup>INSERM, Univ Rennes, INRA, Nutrition Metabolisms and Cancer (NuMeCan), UMR-1241, Rennes, France; <sup>7</sup>Sorbonne Université/Inserm Unité UMRS NutriOmics, Assistance publique hôpitaux de Paris, service de Nutrition, Paris, France

JHEP Reports 2019. <https://doi.org/10.1016/j.jhepr.2019.09.005>

**Background & Aims:** There is an urgent medical need to develop non-invasive tests for non-alcoholic steatohepatitis (NASH). This study evaluates the diagnostic performance of an innovative model based on mid-infrared (MIR) spectroscopy for the diagnosis of NASH.

**Methods:** Severely obese patients who underwent a bariatric procedure at the University Hospital of Nice, France (n = 395) were prospectively recruited. The clinico-biological characteristics were measured prior to surgery. Liver biopsies were collected during the surgical procedure and assessed by a pathologist. A training group (316 patients, NASH: 16.8%) and a validation group (79 patients, NASH: 16.5%) were randomly defined. MIR spectra were acquired by fiber evanescent wave spectroscopy, using chalcogenide glass fiber optic sensors and a spectrometer. This absorption spectroscopic technique delivers a spectrum that identifies the molecular composition of a sample, defining a patient's metabolic fingerprint.

**Results:** The areas under the receiver operating curve (AUROC) for the diagnosis of NASH were 0.82 and 0.77 in the training and validation groups, respectively. The best threshold was 0.15, which was associated with a sensitivity of 0.75 and 0.69, and a specificity of 0.72 and 0.76. Negative predictive values of 0.94 and 0.93 and positive predictive values of 0.35 and 0.36, as well as correctly classified patient rates of 72% and 75% were obtained in the training and validation groups, respectively. A composite model using aspartate aminotransferase level, triglyceride level and waist circumference alongside the MIR spectra led to an increase in AUROC (0.88 and 0.84 for the training and validations groups, respectively).

**Conclusions:** MIR spectroscopy provides good sensitivity and negative predictive values for NASH screening in patients with severe obesity.

© 2019 The Author(s). Published by Elsevier B.V. This is an open access article under the CC BY-NC-ND license (<http://creativecommons.org/licenses/by-nc-nd/4.0/>).

## Introduction

The global epidemic of obesity is responsible for numerous chronic complications including non-alcoholic fatty liver disease (NAFLD).<sup>1</sup> Whereas NAFLD affects up to 25% of the world population, non-alcoholic steatohepatitis (NASH) is present in 1.5–6.45% of the world population.<sup>2</sup> In severely obese individuals, the prevalence of NAFLD can reach 80–92%, with NASH occurring in 15–30% of patients.<sup>3,4</sup> With such a high number of patients, the development of non-invasive markers is needed to effectively screen for liver injury.

Although several non-invasive blood or physical tests (such as measurement of liver stiffness by elastography) have been developed for liver fibrosis over the past 15 years, the non-invasive diagnosis of NASH remains a challenge, especially in routine practice.<sup>5</sup> Currently, no non-invasive test for the screening or the diagnosis of NASH has emerged that has good diagnostic performance.<sup>6</sup> Fibrosis has indeed been shown to be the main predictor of liver-related and global mortality and NASH is well recognized as the main driver of liver fibrosis.<sup>7,8</sup> The presence of NASH is associated with the occurrence of type 2 diabetes (T2D) and cardiovascular complications, which are the main causes of mortality in patients with NAFLD without cirrhosis.<sup>9,10</sup> Thus, there is an urgent medical need to develop non-invasive tests.<sup>6</sup> Indeed, screening for the presence of NASH is of interest even in patients with NAFLD and a low stage of fibrosis. To date, drug development mainly targets patients with overt NASH and significant fibrotic or cirrhotic NASH.<sup>7</sup> However, one can hypothesize that early screening of NASH among patients with NAFLD could lead to early lifestyle modification proposals and help in patient compliance. Indeed, 10% weight loss is well known to improve patient liver condition and decrease cardiometabolic risks.<sup>9,11</sup>

Furthermore, screening for NASH among severely obese patients could provide an indication for bariatric surgery

**Keywords:** Fiber evanescent wave spectroscopy; mid-infrared (MIR) spectroscopy; chalcogenide glass; non-alcoholic steatohepatitis; NASH; severely obese patients; non-invasive test; metabolic fingerprint.

Received 8 May 2019; received in revised form 23 September 2019; accepted 28 September 2019; Available online 23 October 2019

\* Corresponding author. Address: Centre Hospitalier Universitaire de Nice, Digestive Center, 151 route de Saint Antoine de Ginestière, 06202 Nice, France; Tel.: +33 (0) 4 92 03 59 43, fax: +33 (0) 4 92 03 92 39.

E-mail address: [anty.r@chu-nice.fr](mailto:anty.r@chu-nice.fr) (R. Anty).

†Both authors contributed equally to the manuscript.



(BS), since BS has been demonstrated to be beneficial for the liver.<sup>12–14</sup> However, liver biopsy, the sole tool to confirm the diagnosis of NASH, cannot be proposed to all at-risk patients. In the field of non-invasive tests, the main options are blood-based tests and physical tests. An emerging technology with the potential to meet these requirements is based on fiber evanescent wave spectroscopy (FEWS) performed in the mid-infrared (MIR) spectral domain. Ideally, using such technology, screening for NASH should be easily performed by the clinician, easily accepted by the patient, reliable and cost-effective.

FEWS records a broad metabolic profile from a drop of serum that is placed on a chalcogenide glass fiber optic sensor on the basis of a MIR absorption spectrum.<sup>15</sup> MIR spectroscopy is based on the ability of organic molecular chemical bonds to undergo vibrational transition in the MIR region and to generate absorption bands in specific and thus assignable frequency ranges. An evanescent wave is the part of the electromagnetic field that propagates at the surface of a fiber when the infrared (IR) beam is internally reflected at the fiber/air interface; this evanescent wave is absorbed by the chemical groups that are in close contact with the fiber. Thus, merely placing a biological sample in contact with the fiber allows one to resolve an absorption spectrum at the fiber output. The spectrum reflects the organic molecular composition of the whole sample, thus providing a metabolic fingerprint.<sup>16</sup>

Many bio-spectroscopic studies have demonstrated the potential of MIR spectroscopy for medical diagnosis, generally using tissue,<sup>17</sup> yet more recently also using biofluids like serum,<sup>18,19</sup> plasma,<sup>20,21</sup> and tears.<sup>22</sup> In hepatology, pilot studies have unveiled the relevance of MIR spectroscopy for the diagnosis of liver or bile duct cancer, or for the prognostic evaluation of decompensated cirrhosis.<sup>23–27</sup>

The aim of this study was to identify the relevance of FEWS technology to identify obese patients with or without NASH using a comparison approach between this novel technique and liver biopsy-based NASH diagnosis.

## Patients and methods

### Patient inclusion

Three hundred and ninety-five consecutive severely and morbidly obese patients referred for bariatric surgery to the University Hospital of Nice, were included in the study between January 2006 and July 2012. These patients were indicated for bariatric surgery in agreement with French guidelines and the 1991 NIH Consensus Conference guidelines for gastrointestinal surgery for obesity.<sup>28,29</sup> The study protocol was performed according to French legislation regarding Ethics and Human Research and was approved by the local Ethics Committee (Huriet-Serusclet law, DGS 2003/0395). Written informed consent was obtained from all patients. All patients were negative for hepatitis B and C viral markers, for auto-antibodies indicative of autoimmune hepatitis, and had negligible alcohol consumption (<20 g/day in women and <30 g/day in men). Alcohol abuse was also excluded by interviewing the patients' relatives. Patients with a history of inflammatory disease (including rheumatoid arthritis, systemic lupus erythematosus, and inflammatory bowel disease), current infection, a recent history of cancer (<5 years), and severe pulmonary or cardiac disease were not enrolled in the study.

Surgical liver biopsy was obtained during the operation for all patients, as previously reported.<sup>30</sup>

### Preoperative assessment

The data included in this study are issued from a prospective cohort of morbidly obese patients undergoing bariatric surgery at our tertiary bariatric referral center at a time when patients had no preoperative diet restriction, or other preoperative treatments (such as omega-3 fatty acids for example) that may have interfered with the evolution of NAFLD. Clinico-biological preoperative assessment was performed 2 to 3 weeks before surgery and included: a medical history and physical examination, blood pressure analysis, anthropometric measurements (weight, height, waist circumference), psychiatric and nutritional evaluation, blood samples obtained after overnight fasting for determination of plasma levels of alanine aminotransferase (ALT), aspartate aminotransferase (AST), gamma-glutamyltransferase (GGT), glucose, insulin, C-peptide, glycosylated hemoglobin, triglycerides, high-density lipoprotein (HDL) cholesterol, and low-density lipoprotein (LDL) cholesterol. ALT and AST levels were determined using the Roche assay with pyridoxal phosphate on a Hitachi Modular according to the International Federation of Clinical Chemistry and the Société Française de Biologie Clinique recommendations. In our center, the upper limit of normal ALT was 31 IU/L for women and 41 IU/L for men. Glycosylated hemoglobin was determined with the Biorad Dual kit A1c on a Variant 2 Biorad (Biorad, USA). All patients also had a chest X-ray, electrocardiogram, abdominal ultrasound and upper gastrointestinal endoscopy. Metabolic syndrome was defined as the presence of at least 3 of the following parameters: elevated waist circumference ( $\geq 94$  cm in men or  $\geq 80$  cm in women), elevated blood pressure (systolic blood pressure  $\geq 130$  mmHg or diastolic blood pressure  $\geq 85$  mmHg or antihypertensive drug), elevated blood glucose ( $\geq 100$  mg/dl or anti-diabetic drug), elevated triglycerides ( $\geq 150$  mg/dl or lipid-lowering drug), and low HDL cholesterol (<40 mg/dl in men or <50 mg/dl in women or lipid-lowering drug).<sup>31</sup> Notably, all obese patients who were candidates for bariatric surgery had a waist circumference above the defined threshold for metabolic syndrome. Type 2 diabetes was defined by 2 elevated measurements for fasting plasma glucose  $\geq 7$  mmol/L. Serum was collected from each patient and immediately stored at  $-80^{\circ}\text{C}$ .

### Liver assessment

Hepatic wedges were obtained during bariatric surgery by surgeons specialized in liver surgery and transplantation (AI and JG). Hepatic wedges were at least 10 mm long. Surgical liver biopsies were reviewed by 1 liver pathologist (SP), blinded regarding the clinical or biological characteristics of the patients. Routine haematoxylin-eosin-safran and Sirius red staining was performed on all biopsies. Biopsies were graded according to the NAFLD activity score (NAS)<sup>33</sup> and the steatosis, activity and fibrosis (SAF) score.<sup>34</sup> The diagnosis of NASH was retained in patients with steatosis grade  $\geq 1$  + lobular inflammation grade  $\geq 1$  + ballooning grade  $\geq 1$  (according to the SAF score). Liver fibrosis was assessed by Sirius red staining and was classified into 7 stages according to the NASH Clinical Research Network Scoring System Definition and Scores as follows: F0: no fibrosis, F1a: mild zone 3 sinusoidal fibrosis, F1b: moderated zone 3 sinusoidal fibrosis, F1c: peri-portal sinusoidal fibrosis, F2: zone 3 sinusoidal fibrosis and peri-portal sinusoidal fibrosis, F3: bridging fibrosis, F4: cirrhosis.<sup>32,34</sup>

**Follow-up cohort**

Ten patients with NASH at baseline, as determined by liver biopsy, were contacted and had an additional liver biopsy to follow changes in the liver pathology after bariatric surgery. Clinico-biological data and serum were collected at the time of the follow-up liver biopsy. Diagnostic performance of the MIR spectroscopy was also assessed.

**Fiber evanescent wave spectroscopy**

*Acquisition of spectra*

The MIR spectra were recorded using a DIAFIR SPID™ FT-IR spectrometer (Rennes - France). The FTIR absorption spectra were acquired in the 4,000–600 cm<sup>-1</sup> frequency range. The nominal spectral resolution was set to 4 cm<sup>-1</sup> and a zero-filling factor of 2 was employed, yielding a discrete spectral point spacing of 2 cm<sup>-1</sup>. A Blackman Harris 3-term apodization function was used for Fourier transformation. For each spectrum, 64 scans were co-added.

For spectral acquisition, a disposable FEWS infrared sensor was placed in the spectrometer, the background signal was recorded in air, and 7 µl of serum was deposited on the sensor. The serum spectrum was acquired 8 min after deposition to obtain an accurate signal and remove excess water that can screen some infrared bands of interest.

All measures were made on thawed sera samples collected before surgery.

*Pre-treatments*

MIR spectra were pre-processed and analyzed in the 3,800–950 cm<sup>-1</sup> frequency domain, where most of the biomolecules are apparent. Several signal quality parameters (signal intensity, signal to noise ratio, water vapor) were measured and validated, and data homogeneity (outlier identification) was visually checked. A straight line was generated from 2,800 to 1,800 cm<sup>-1</sup> to eliminate the contribution of environmental CO<sub>2</sub>. Second derivatives were calculated, smoothed using a 13-point Savitzky-Golay smoothing algorithm, and vector normalized over the whole spectral range.

**Statistical analysis of spectra**

The statistical analyses of spectra aimed to discriminate patients without NASH from those with NASH.

Spectral analysis required the number of spectral variables (*i.e.*, wavenumbers) to be reduced from a few hundred to approximately a dozen, to minimize the influence of noisy and/or redundant variables. The population was randomly separated into 2 groups: the training group (4/5 of the cohort, 316 patients) and the validation group (1/5 of the cohort, 79 patients) and the sets were compared to make sure that there were no significant differences in clinical and histological features (Table 1). Wavenumber selection and optimization were performed with the sole training group to limit the overlearning risk. The spectroscopic curves (vector normalized second derivatives) were first projected on a Spline basis to reduce the dimension of the data and smooth the curves. Variable selection was then performed on the Spline coefficients, with a stability selection procedure based on repetition of random forest variable selection<sup>35</sup> with subsamples of the training set. For each run of the stability selection procedure a subsample containing 4/5 individuals from the training set was selected and a random forest regression performed. The most important variables, according to the decrease in the Gini index (a multivariate measure of variable importance

**Table 1. Characteristics of the patients in the training and validation groups.**

	Patients in the training group (n = 316)	Patients in the validation group (n = 79)	p value
Age (years)	40 (31–48)	41 (34–48)	0.4
Weight (kg)	117 (107–131)	113 (104–128)	0.2
BMI (kg/m <sup>2</sup> )	44 (41–47)	43 (40–47)	0.3
AST (IU/L)	24 (20–30)	24 (21–35)	0.5
ALT (IU/L)	27 (19–41)	24 (19–36)	0.6
GGT (IU/L)	31 (20–50)	28 (19–49)	0.5
Blood glucose level (mmol/L)	5.2 (4.8–6.1)	5.3 (4.9–5.8)	0.7
Insulin (mmol/L)	19 (13–27)	18 (11–23)	0.08
HbA1c (%)	5.6 (5.4–6)	5.6 (5.3–6.1)	0.4
Total cholesterol (mmol/L)	5.3 (4.6–6.1)	5.4 (4.7–6)	0.9
HDL cholesterol (mmol/L)	1.3 (1.2–1.6)	1.4 (1.2–1.7)	0.4
LDL cholesterol (mmol/L)	3.2 (2.6–3.8)	3.2 (2.6–3.8)	0.8
Triglyceride (mmol/L)	1.5 (1.1–2.2)	1.3 (1–1.9)	0.1
Waist circumference (cm)	120 (120–128)	117 (116–125)	0.06
Type 2 diabetes presence (%)	20	23	0.7
Metabolic Syndrome presence (%)	50	42	0.2
Steatosis (%), S0-S1-S2-S3	6-40-26-28	8-37-29-26	0.9
Ballooning (%), B0-B1-B2	80.4-19.3-0.3	81-16.5-2.5	0.1
Inflammation (%), I0-I1-I2	83-16-1	82-18-0	0.8
No NASH/NASH (%)	83.2/16.8	83.5/16.5	1
Fibrosis (%), F0-F1-F2-F3	13.1-61.7-19.8-5.4	16.7-62.8-16.7-3.8	0.7

ALT, alanine aminotransferase; AST, aspartate aminotransferase; BMI, body mass index; GGT, gamma-glutamyltransferase; HbA1c, glycated hemoglobin; HDL, high-density lipoprotein; LDL, low-density lipoprotein; NASH, non-alcoholic steatohepatitis. Quantitative values are displayed as median and interquartile range.

of the random forest), were collected.<sup>36</sup> These steps were repeated 200 times, and the variables that were finally retained were those with the highest probability of selection. Once the optimized wavenumber set (20 variables) was defined, a mixture of a logistic regression model was built using this set with the training population, and the performance was checked on the validation population.

The best threshold was that which provided the best association between sensitivity and specificity for the screening of NASH. All the statistical analyses were performed with the R statistical software. Algorithm performances of the MIR spectroscopy model were estimated according to the area under the ROC curve (AUROC), sensibility, specificity, negative predictive values and positive predictive values at the best threshold.

**Elaboration of a model using clinico-biological and spectral data to diagnose NASH**

Clinical and biological variables are given as the median and the standard deviation. All variables were tested for a normal distribution with the Shapiro-Wilk test. Comparisons were made using the Student's *t* test for normally distributed data or with the Mann-Whitney *U* test. Nominal data were tested using the

Fisher's exact test. A logistic regression analysis based on variables significantly associated with NASH was conducted using a univariate analysis ( $p < 0.05$ ). Patients with missing clinical parameter data were not included in the multivariate model. The clinico-biological data independently associated with NASH were used to calculate a clinical model. Moreover, these clinico-biological data were used with the score obtained on the spectral analysis to construct a new model to diagnose NASH (composite model). Comparisons of the AUROCs were made using Delong's tests<sup>37</sup> and bootstrap sampling.

All the statistical analyses were performed with the R statistical software.

## Results

### Characteristics of the patients

Three hundred and ninety-five patients were included. Sixty-six of these patients had NASH (17%). The cohort was randomly split into 2 groups to obtain a training group (4/5 of the overall cohort, including 53 patients with NASH and 263 patients without NASH) and a validation group (1/5 of the overall cohort, including 13 patients with NASH and 66 patients without NASH). As mentioned in the patients and method section, the training and validation groups were similar for all clinico-biological variables (Table 1). The patient characteristics of the overall cohort are shown in Table 2.

**Table 2. Characteristics of the severely obese patients in the entire cohort.**

	Patients with NASH (n = 66)	Patients without NASH (n = 329)	p value
Age (years)	43 (38–51)	39 (31–47)	4.10 <sup>-3</sup>
Weight (kg)	123 (110–135)	114 (106–129)	0.02
BMI (kg/m <sup>2</sup> )	44 (42–48)	43 (41–47)	0.15
AST (IU/L)	35 (26–44)	23 (19–29)	5.10 <sup>-9</sup>
ALT (IU/L)	43 (28–64)	24 (18–36)	2.10 <sup>-8</sup>
GGT (IU/L)	54 (30–81)	28 (19–45)	8.10 <sup>-8</sup>
Blood glucose level (mmol/L)	5.7 (5–8)	5.2 (4.8–5.8)	3.10 <sup>-4</sup>
Insulin (mmol/L)	23 (15–33)	18 (11–25)	6.10 <sup>-4</sup>
HbA1c (%)	6 (5.5–7.2)	5.6 (5.3–5.9)	2.10 <sup>-6</sup>
Total cholesterol (mmol/L)	5.2 (4.5–6.1)	5.4 (4.7–6)	0.8
HDL cholesterol (mmol/L)	1.2 (1.1–1.5)	1.4 (1.2–1.6)	5.10 <sup>-3</sup>
LDL cholesterol (mmol/L)	2.9 (2.4–3.7)	3.2 (2.6–3.8)	0.04
Triglyceride (mmol/L)	1.7 (1.1–2.9)	1.4 (1.1–1.9)	9.10 <sup>-4</sup>
Waist circumference (cm)	127 (126–134)	118 (117–125)	1.10 <sup>-6</sup>
Type 2 diabetes presence (%)	38	17	3.10 <sup>-4</sup>
Steatosis (%), S0-S1-S2-S3	72	46	4.10 <sup>-4</sup>
Ballooning (%), B0-B1-B2	0-8-32-60	7-46-26-21	4.10 <sup>-12</sup>
Inflammation (%), I0-I1-I2	0-95-5	97-3-0	10 <sup>-16</sup>
Steatosis (%), S0-S1-S2-S3	0-97-3	99-1-0	10 <sup>-16</sup>
Fibrosis (%), F0-F1-F2-F3	15.4-52.3-16.9-15.4	13.5-63.8-19.6-3.1	5.10 <sup>-3</sup>

ALT, alanine aminotransferase; AST, aspartate aminotransferase; BMI, body mass index; GGT, gamma-glutamyltransferase; HbA1c, glycated hemoglobin; HDL, high-density lipoprotein; LDL, low-density lipoprotein; NASH, non-alcoholic steatohepatitis. Quantitative values are displayed as median and interquartile range.

As expected, AST, ALT, GGT, blood glucose, insulin, glycosylated hemoglobin, triglyceride level, waist circumference and the prevalence of metabolic syndrome were higher in patients with NASH compared to patients without NASH. HDL cholesterol levels were lower in patients with NASH compared to patients without NASH. The grade of steatosis and stage of fibrosis were higher in patients with NASH.

### Diagnostic performance of MIR spectroscopy for the diagnosis of NASH in severely obese patients at the time of surgery

When comparing histological diagnosis of NASH to that obtained by MIR spectroscopy, the AUROC for the diagnosis of NASH were 0.82 and 0.77 for the training and validation groups, respectively (Fig. S1). The best threshold was 0.15, which was associated with a sensitivity of 0.75 and 0.69, and a specificity of 0.72 and 0.76, negative predictive values of 0.94 and 0.93, positive predictive values of 0.35 and 0.36. Finally, correctly classified patient rates of 72% and 75% were obtained for the training and validation groups, respectively (Table 3).

### Association of the MIR spectroscopic score with the severity of liver pathology

We next analyzed, in each group, the relationship between the MIR technology-based score and individual histological lesions defining NASH – steatosis, inflammation, ballooning – as well as with the NAS and the fibrosis level (Fig. 1).

In the training group, despite large inter-individual variability, the MIR spectroscopic score was significantly higher in patients with steatosis S2 and S3 as compared to S0 and S1 (Fig. 1A). The MIR technology score was also significantly higher in patients with either grade 1 or grade 2 inflammation compared to grade 0 (Fig. 1B), as well as in patients with grade 1 ballooning compared to grade 0 (Fig. 1C). A significantly higher MIR technology score was also found in patients with NAS  $\geq 5$  compared to patients with  $3 \leq \text{NAS} < 5$ , and with NAS  $< 3$ ; and in patients with  $3 \leq \text{NAS} < 5$  compared to patients with NAS  $< 3$  (Fig. 1D), as well as in patients with fibrosis grade 3 compared to grades 2, 1 and 0 (Fig. 1E).

In the validation group, similar observations were made except for fibrosis, probably because of the limit number of patients in each stage (Fig 1F-J).

### Diagnostic performance of spectroscopy for NASH after surgery

The model was also applied to a group of 10 severely obese patients treated with laparoscopic Roux-en-Y gastric-by-

**Table 3. Diagnostic performance of MIR spectroscopy for the diagnosis of NASH in severely obese patients at the time of the surgery.**

	Patients in the training group (n = 316)	Patients in the validation group (n = 79)
AUROC	0.82	0.77
Sensitivity	0.75	0.69
Specificity	0.72	0.76
Negative predictive value	0.94	0.93
Positive predictive value	0.35	0.36
Correctly classified patients (%)	72	75

AUROC, area under the receiver operating curve; MIR, mid-infrared; NASH, non-alcoholic steatohepatitis. Pure spectral model, at the best threshold (0.15).

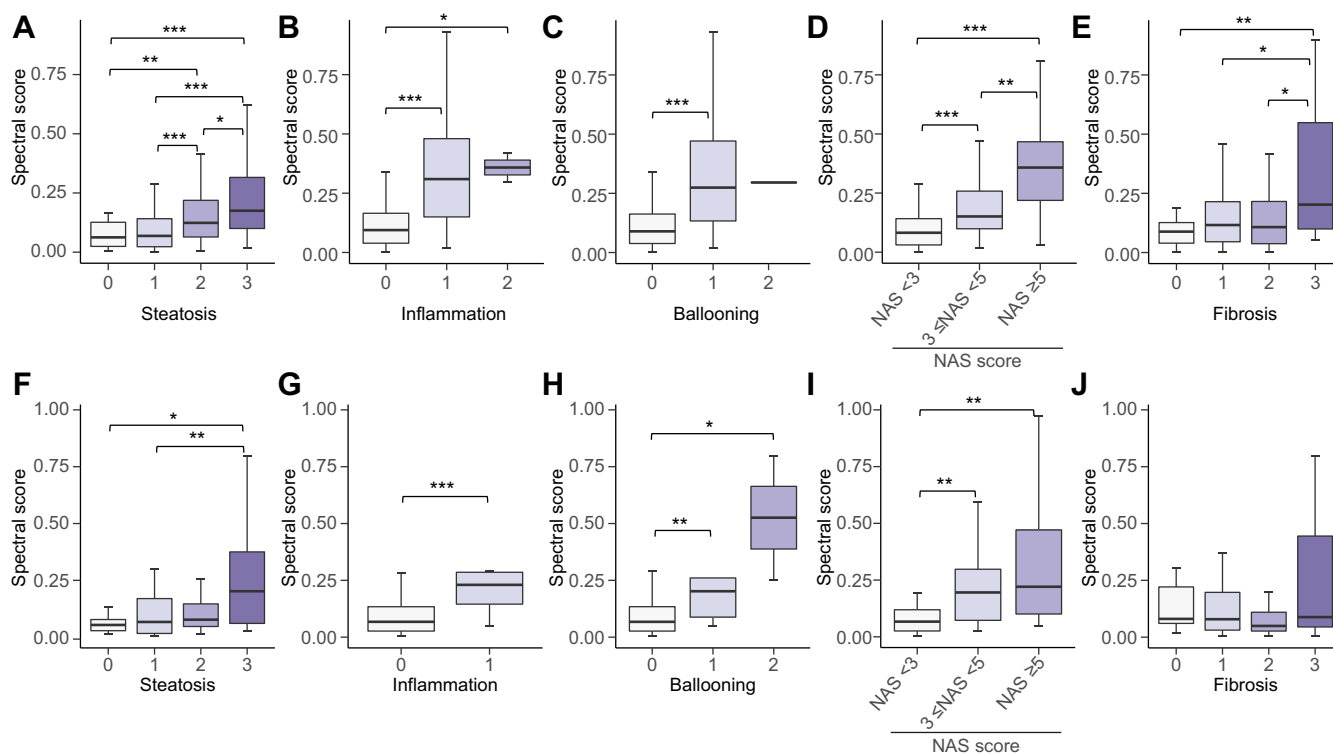


**Fig. 1. Association of the MIR spectroscopic values with the severity of liver pathology, for the training and the validation groups.** (A-E) Training group, various grades of (A) steatosis; (B) inflammation; (C) ballooning; (D) NAFLD activity score; and (E) fibrosis are represented. (F-J) Validation group, various grades of (F) steatosis; (G) inflammation; (H) ballooning; (I) NAFLD activity score; and (J) fibrosis are represented. To facilitate visualization, outliers are not represented; see method for details regarding the liver pathology analysis. MIR, mid-infrared; NAFLD, non-alcoholic fatty liver disease.

pass who were followed for 5 (3–6.5) years after surgery. Clinico-biological data and liver pathology at baseline, and at the time of the liver biopsy, are shown in Table S1. Initially all patients had NASH. At the time of the additional biopsy, only 1 patient had persistent NASH. The AUROC of the model was 0.81. The only patient with NASH was correctly classified. Among the 9 patients without NASH, 5 were correctly classified (Table S2).

The individual variations of spectroscopy results in these 10 patients are presented in Fig. 2.

**Diagnostic performance of a composite model including spectroscopic and clinico-biological data**

To improve the diagnostic performance, a new composite model was computed that also took clinico-biological data into account. The multivariate analysis and the clinical variable selection for the diagnosis of NASH were performed on the calibration set (see Table S3 for details of the differences between patients with or without NASH for the calibration set). Using a logistic regression model, the AST, triglyceride level and waist circumference were included, as they were the only independent parameters that were significantly associated with NASH in the training group (Table S4). The diagnostic values of a clinico-biological model that only used these 3 parameters are presented in Table S5. A new composite model was therefore computed to diagnose NASH. The diagnostic performance is displayed in Table 4. The AUROC were 0.88 and 0.84 for the training and validation groups,

respectively (Fig. S2). The best threshold was 0.13, which was associated with sensitivities of 0.80 and 0.67, specificities of 0.79 and 0.80, negative predictive values of 0.95 and 0.93, positive predictive values of 0.43 and 0.38, as well as correctly classified patient rates of 79% and 78% for the training and validation groups, respectively. Even if the AUROC were slightly higher in this composite model (0.88 and 0.84), compared to the sole spectral model (0.82 and 0.77), there was no statistical difference between them for the validation set ( $p = 0.09$ ) due to the small sample size. However, we noted that there was a significant difference between the AUROC of these 2 models for the calibration set ( $p = 0.02$ ). The bootstrap sampling confirmed these results (Table S6).

**Discussion**

This clinical study using a newly developed technology demonstrated that FEWS performed in the MIR spectral domain is an encouraging method for the non-invasive diagnose of NASH in obese patients. The diagnostic performance, with good sensitivity and a very good negative predictive value, suggests that MIR technology could be used in routine care as a screening test for NASH.

Development of non-invasive tests for patients with NAFLD/NASH remains a major challenge.<sup>6,38</sup> Although numerous tests have been proposed for non-invasive assessment of fibrosis, no satisfactory test has yet been developed for the diagnosis and screening of NASH.<sup>6,38</sup>

In this context, FEWS performed with MIR provides several benefits: it is minimally invasive, easy both to perform and to interpret for the clinician, and provides a quick answer, almost at the bedside. Easy and rapid screening for NASH with this sensitive test offers several advantages, in the new area of personalized medicine: i) it identifies patients at a low risk of NASH, thus enabling clinicians to reassure these patients and propose a lighter follow-up dedicated towards prevention and efforts to control cardiovascular risk factors, which will also avoid non-useful and potentially expensive complementary liver tests for these patients; ii) it will enable clinicians to focus on more aggressive care for patients diagnosed with NASH.

It might be anticipated that in the future, the MIR technology should be associated with other non-invasive tests dedicated to screening for the presence and/or severity of fibrosis in patients diagnosed with “NASH”, since MIR technology displayed poor specificity and a low positive predictive value. For example, common liver fibrosis tests such as FIB-4 or the NAFLD fibrosis score, or the measurement of liver stiffness by elastography, could be performed to identify patients at a high risk of fibrotic NASH.<sup>39</sup> The precise potential contribution of the MIR spectroscopy model to the algorithm for the diagnosis of NASH and NASH with fibrosis will have to be determined in the future. The lack of a strong positive predictive value is a critical issue in non-invasive test development for fibrosis particularly for intermediate stages of fibrosis.<sup>39</sup> We combined clinico-biological variables to the spectral ones to improve the MIR spectroscopy model. Although we did not succeed in significantly improving the positive predictive value, we observed a significant difference between the AUROC of these 2 models, for the diagnosis of NASH, for the calibration set (0.88 vs. 0.82;  $p = 0.02$ ). Moreover, the distribution of the AUROC values according to the bootstrap sampling showed that the performance of the composite model was higher and less variable.

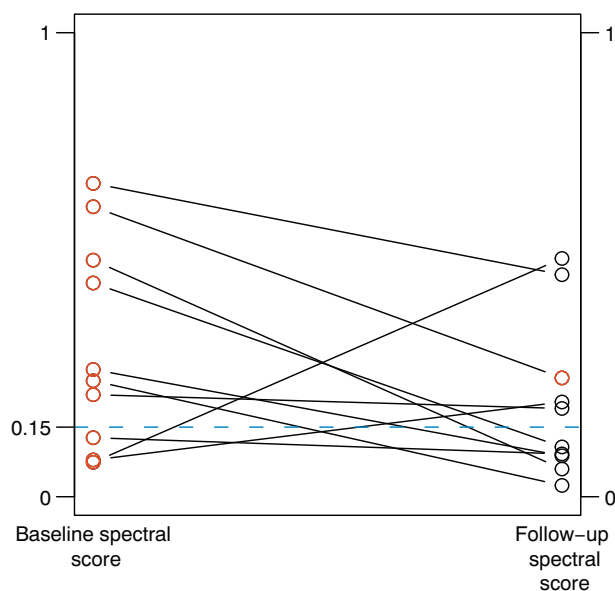


**Fig. 2. Individual variations of spectroscopy results in the 10 severely obese patients from the follow-up cohort.** Circle in red: patients with NASH; circle in black: patients without NASH; Blue dash line: threshold of the spectral model. NASH, non-alcoholic steatohepatitis.

**Table 4. Diagnostic performance of a multivariate model for the diagnosis of NASH in severely obese patients at the time of surgery.**

	Patients in the training group (n = 297)	Patients in the validation group (n = 77)
AUROC	0.88	0.84
Sensitivity	0.8	0.67
Specificity	0.79	0.8
Negative predictive value	0.95	0.93
Positive predictive value	0.43	0.38
Correctly classified patients (%)	79	78

Mixed model associating spectral data with clinico-biological data for the diagnosis of NASH at the best threshold (0.13). AUROC, area under the receiver operating curve; NASH, non-alcoholic steatohepatitis.

The lack of positive predictive values probably originates from the low prevalence of patients with NASH in our cohort (17%), nevertheless concordant with other series studying severely obese patients referred for bariatric surgery.<sup>40</sup> This relatively low prevalence is particularly challenging for a diagnostic test.

This study is then the first to demonstrate the potential for FEWS to be performed with MIR for the diagnosis of NASH in severely obese patients. This is a monocentric study performed on a large number of well-characterized patients. All patients had a liver biopsy assessed by 1 pathologist (SP), which is the reference examination to classify the severity of NAFLD. A robust spectral method has been implemented to yield a model that allows patients with and without NASH to be detected using training and validation groups. Based on the current study, assessing the relationships between the different hepatic lesions and the MIR spectroscopic score, our data support the idea that serum metabolic alterations associated with inflammation and ballooning are critical in determining the score. This finding reinforces the potential interest of the test for the follow-up of patients and is in line with data that we obtained from the group of patients for whom the histological studies after post-bariatric surgery evolved in parallel to the decreasing score.

We nevertheless have a number of challenges to address. The relevance of this technology will have to be replicated and externally validated in several independent cohorts of severely obese patients. Accordingly, a European multicentric prospective study of severely obese patients is being developed to validate this technology and will start recruitment in the near future (NCT 03978247). Of course, validation in populations of patients with NAFLD outside bariatric surgery is required before transfer to clinical practice. So, the tests have to be extended for the diagnosis of NASH in overweight and moderately obese patients who represent most of the patients seen by hepatologists. Its interest in the sequential or parallel association with other non-invasive tests for fibrosis or fibrotic NASH screening will have to be defined. Finally, its potential interest for patients in diabetic clinics and/or in the general population will have to be assessed. Interestingly in our cohort, T2D status did not improve nor change the accuracy of this new non-invasive tool, suggesting that it could adequately screen for NASH in patients T2D.

In conclusion, MIR-FEWS offers new opportunities to non-invasively assess the liver of severely obese patients, thereby providing a sensitive test to screen for NASH. Further multicentric stu-

dies are required to complete the clinical validation of this technology and to confirm its potential as a non-invasive test to detect NASH.

### Abbreviations

ALT, alanine aminotransferase; AST, aspartate aminotransferase; AUROC, area under the receiver operating curve; BMI, body mass index; FEWS, fiber evanescent wave spectroscopy; FTIR, Fourier transform infrared; GGT, gamma-glutamyltransferase; HbA1c, glycated hemoglobin; HDL, high-density lipoprotein; HOMA-IR, homeostasis model assessment of insulin resistance; IR, infrared, LDL, low-density lipoprotein; MIR, mid-infrared; NAFLD, non-alcoholic fatty liver disease; NAS, NAFLD activity score; NASH, non-alcoholic steatohepatitis; SAF, steatosis, activity and fibrosis; T2D, type 2 diabetes.

### Financial support

This work was supported by grants from INSERM (France), Université Nice Sophia-Antipolis, PHRC (Centre Hospitalier Universitaire de Nice), Association Française pour l'Etude du Foie (AFEF)/LFB to PG, AFEF/Aptalis to BBM, Société Francophone du Diabète (SFD) to PG, SFD/Roche Pharma to PG, and SFD/MSD to BBM. This work was also funded by the French Government (National Research Agency, ANR): #ANR-15-CE14-0016-01, #ANR-18-CE14-0019-02, the Investments for the Future LABEX SIGNALIFE (#ANR-11-LABX-0028-01) and the UCA<sup>JEDI</sup> Investments in the Future project (#ANR-15-IDEX-01).

### Conflict of interest

Rodolphe Anty, Clémence M Canivet, Stéphanie Patouraux, Jean Gugenheim, Stéphanie Bonnafous, Béatrice Bailly-Maitre, Thierry Piche, Olivier Sire, Judith Aron-Wisniewsky, Karine Clément, Albert Tran, Antonio Iannelli, Philippe Gual have nothing to disclose; Marie Morvan is a service provider for DIAFIR; Maëna Le Corvec is a DIAFIR employee; Jérôme Bernard is the DIAFIR General Manager for Healthcare; Hugues Tariel is the DIAFIR Chief Executive Officer; Olivier Loréal is a DIAFIR co-founder.

Please refer to the accompanying ICMJE disclosure forms for further details.

### Authors' contributions

OL, HT, OS developed the concept; MM, MLC, RA obtained data; RA, MM, MLC, JB, designed the study; RA, MM, MLC wrote the manuscript; MM performed the statistical analysis; RA, AI, JG, TP recruited patients; RA, CMC, SP, SB, BBM managed clinico-biological data and samples; PG, OL, AT, AI, JAW, KC provided critical reading of the manuscript and all other co-authors approved the paper.

### Acknowledgments

Our thanks to Abby Cuttriss from the Office of International Scientific Visibility for comments on the English version of the manuscript.

### Supplementary data

Supplementary data associated with this article can be found, in the online version, at <https://doi.org/10.1016/j.jhepr.2019.09.005>.

### References

- [1] Ng M, Fleming T, Robinson M, Thomson B, Graetz N, Margono C, et al. Global, regional, and national prevalence of overweight and obesity in children and adults during 1980–2013: a systematic analysis for the Global Burden of Disease Study 2013. *Lancet* 2014;384:766–781.
- [2] Younossi ZM, Koenig AB, Abdelatif D, Fazel Y, Henry L, Wymer M. Global epidemiology of nonalcoholic fatty liver disease—Meta-analytic assessment of prevalence, incidence, and outcomes. *Hepatology* 2016;64:73–84.

- [3] Anty R, Marjoux S, Iannelli A, Patouraux S, Schneck AS, Bonnafous S, et al. Regular coffee but not espresso drinking is protective against fibrosis in a cohort mainly composed of morbidly obese European women with NAFLD undergoing bariatric surgery. *J Hepatol* 2012;57:1090–1096.
- [4] Bedossa P, Tordjman J, Aron-Wisniewsky J, Poitou C, Oppert J-M, Torcivia A, et al. Systematic review of bariatric surgery liver biopsies clarifies the natural history of liver disease in patients with severe obesity. *Gut* 2017;66:1688–1696.
- [5] Eddowes PJ, Sasso M, Allison M, Tsochatzis E, Anstee QM, Sheridan D, et al. Accuracy of FibroScan Controlled Attenuation Parameter and Liver Stiffness Measurement in Assessing Steatosis and Fibrosis in Patients With Nonalcoholic Fatty Liver Disease. *Gastroenterology* 2019 May;156:1717–1730.
- [6] Castera L, Friedrich-Rust M, Loomba R. Non-Invasive Assessment of Liver Disease in Patients with NAFLD. *Gastroenterology* 2019 Apr;156:1264–1281.
- [7] Friedman SL, Neuschwander-Tetri BA, Rinella M, Sanyal AJ. Mechanisms of NAFLD development and therapeutic strategies. *Nat Med* 2018;24:908–922.
- [8] Angulo P, Kleiner DE, Dam-Larsen S, Adams LA, Bjornsson ES, Charatcharoenwitthaya P, et al. Liver Fibrosis, but No Other Histologic Features, Is Associated With Long-term Outcomes of Patients With Nonalcoholic Fatty Liver Disease. *Gastroenterology* 2015;149:389–397.
- [9] Francque SM, van der Graaff D, Kwanten WJ. Non-alcoholic fatty liver disease and cardiovascular risk: Pathophysiological mechanisms and implications. *J Hepatol* 2016;65:425–443.
- [10] Vilar-Gomez E, Calzadilla-Bertot L, Wai-Sun Wong V, Castellanos M, Aller-de la Fuente R, Metwally M, et al. Fibrosis Severity as a Determinant of Cause-Specific Mortality in Patients With Advanced Nonalcoholic Fatty Liver Disease: A Multi-National Cohort Study. *Gastroenterology* 2018;155:443–457.
- [11] Romero-Gómez M, Zelber-Sagi S, Trenell M. Treatment of NAFLD with diet, physical activity and exercise. *J Hepatol* 2017;67:829–846.
- [12] Mathurin P, Gonzalez F, Kerdraon O, Leteurtre E, Arnalsteen L, Hollebecque A, et al. The evolution of severe steatosis after bariatric surgery is related to insulin resistance. *Gastroenterology* 2006;130:1617–1624.
- [13] Mathurin P, Hollebecque A, Arnalsteen L, Buob D, Leteurtre E, Caiazza R, et al. Prospective study of the long-term effects of bariatric surgery on liver injury in patients without advanced disease. *Gastroenterology* 2009;137:532–540.
- [14] Lassailly G, Caiazza R, Buob D, Pigeire M, Verkindt H, Labreuche J, et al. Bariatric Surgery Reduces Features of Nonalcoholic Steatohepatitis in Morbidly Obese Patients. *Gastroenterology* 2015;149:379–388.
- [15] Keirsse J, Lahaye E, Bouter A, Dupont V, Boussard-Plédel C, Bureau B, et al. Mapping bacterial surface population physiology in real-time: infrared spectroscopy of *Proteus mirabilis* swarm colonies. *Appl Spectrosc* 2006;60:584–591.
- [16] Anne M-L, Le Lan C, Monbet V, Boussard-Plédel C, Ropert M, Sire O, et al. Fiber evanescent wave spectroscopy using the mid-infrared provides useful fingerprints for metabolic profiling in humans. *J Biomed Opt* 2009;14:054033.
- [17] Kallenbach-Thieltges A, Großerüschkamp F, Mosig A, Diem M, Tannapfel A, Gerwert K. Immunohistochemistry, histopathology and infrared spectral histopathology of colon cancer tissue sections. *J Biophotonics* 2013;6:88–100.
- [18] Ollesch J, Heinsch M, Heise HM, Behrens T, Brüning T, Gerwert K. It's in your blood: spectral biomarker candidates for urinary bladder cancer from automated FTIR spectroscopy. *J Biophotonics* 2014;7:210–221.
- [19] Hands JR, Dorling KM, Abel P, Ashton KM, Brodbelt A, Davis C, et al. Attenuated total reflection fourier transform infrared (ATR-FTIR) spectral discrimination of brain tumour severity from serum samples. *J Biophotonics* 2014;7:189–199.
- [20] Barlev E, Zelig U, Bar O, Segev C, Mordechai S, Kapelushnik J, et al. A novel method for screening colorectal cancer by infrared spectroscopy of peripheral blood mononuclear cells and plasma. *J Gastroenterol* 2016;51:214–221.
- [21] Peuchant E, Richard-Harston S, Bourdel-Marchasson I, Dartigues J-F, Letenneur L, Barberger-Gateau P, et al. Infrared spectroscopy: a reagent-free method to distinguish Alzheimer's disease patients from normal-aging subjects. *Transl Res* 2008;152:103–112.

Author names in bold designate shared co-first authorship



- [22] Travo A, Paya C, Délérés G, Colin J, Mortemousque B, Forfar I. Potential of FTIR spectroscopy for analysis of tears for diagnosis purposes. *Anal Bioanal Chem* 2014;406:2367–2376.
- [23] Thumanu K, Sangrajang S, Khuhaprema T, Kalalak A, Tanthanuch W, Pongpiachan S, et al. Diagnosis of liver cancer from blood sera using FTIR microspectroscopy: a preliminary study. *J Biophotonics* 2014;7:222–231.
- [24] Zhang X, Thiéfin G, Gobinet C, Untereiner V, Taleb I, Bernard-Chabert B, et al. Profiling serologic biomarkers in cirrhotic patients via high-throughput Fourier transform infrared spectroscopy: toward a new diagnostic tool of hepatocellular carcinoma. *Transl Res* 2013;162:279–286.
- [25] Untereiner V, Sockalingum GD, Garnotel R, Gobinet C, Ramaholimihaso F, Ehrhard F, et al. Bile analysis using high-throughput FTIR spectroscopy for the diagnosis of malignant biliary strictures: a pilot study in 57 patients. *J Biophotonics* 2014;7:241–253.
- [26] Baker MJ, Hussain SR, Lovergne L, Untereiner V, Hughes C, Lukaszewski RA, et al. Developing and understanding biofluid vibrational spectroscopy: a critical review. *Chem Soc Rev* 2016;45:1803–1818.
- [27] Le Corvec M, Jezequel C, Monbet V, Fatih N, Charpentier F, Tariel H, et al. Mid-infrared spectroscopy of serum, a promising non-invasive method to assess prognosis in patients with ascites and cirrhosis. *PLoS ONE* 2017 Oct 11;12:e0185997.
- [28] HAS. *Prise en charge HAS de l'obésité : prise en charge chirurgicale.* [https://www.has-sante.fr/portail/jcms/c\\_765529/fr/obesite-prise-en-charge-chirurgicale-chez-l-adulte](https://www.has-sante.fr/portail/jcms/c_765529/fr/obesite-prise-en-charge-chirurgicale-chez-l-adulte).
- [29] NIH conference. Gastrointestinal surgery for severe obesity. Consensus Development Conference Panel. *Ann Intern Med* 1991;115:956–961.
- [30] Anty R, Iannelli A, Patouraux S, Bonnafous S, Lavallard VJ, Senni-Buratti M, et al. A new composite model including metabolic syndrome, alanine aminotransferase and cytokeratin-18 for the diagnosis of non-alcoholic steatohepatitis in morbidly obese patients. *Aliment Pharmacol Ther* 2010;32:1315–1322.
- [31] Alberti KG, Eckel RH, Grundy SM, Zimmet PZ, Cleeman JJ, Donato KA, et al. Harmonizing the metabolic syndrome: a joint interim statement of the International Diabetes Federation Task Force on Epidemiology and Prevention; National Heart, Lung, and Blood Institute; American Heart Association; World Heart Federation; International Atherosclerosis Society; and International Association for the Study of Obesity. *Circulation* 2009;120:1640–1645.
- [32] Brunt EM, Janney CG, Di Bisceglie AM, Neuschwander-Tetri BA, Bacon BR. Nonalcoholic steatohepatitis: a proposal for grading and staging the histological lesions. *Am J Gastroenterol* 1999;94:2467–2474.
- [33] Kleiner DE, Brunt EM, Van Natta M, Behling C, Contos MJ, Cummings OW, et al. Design and validation of a histological scoring system for nonalcoholic fatty liver disease. *Hepatology* 2005;41:1313–1321.
- [34] Bedossa P, Poitou C, Veyrie N, Bouillot JL, Basdevant A, Paradis V, et al. Histopathological algorithm and scoring system for evaluation of liver lesions in morbidly obese patients. *Hepatology* 2012;56:1751–1759.
- [35] Menze BH, Petrich W, Hamprecht FA. Multivariate feature selection and hierarchical classification for infrared spectroscopy: serum-based detection of bovine spongiform encephalopathy. *Anal Bioanal Chem* 2007;387:1801–1807.
- [36] Breiman L, Friedman JH, Olshen RA, Stone CJ. *Classification and Regression Trees*. Belmont, California: Wadsworth, 1984.
- [37] DeLong ER, DeLong DM, Clarke-Pearson DL. Comparing the areas under two or more correlated receiver operating characteristic curves: a non-parametric approach. *Biometrics* 1988;44:837–845.
- [38] Machado MV, Cortez-Pinto H. Non-invasive diagnosis of non-alcoholic fatty liver disease. A critical appraisal. *J Hepatol* 2013;58:1007–1019.
- [39] Boursier J, Vergniol J, Guillet A, Hiriart J-B, Lannes A, Le Bail B, et al. Diagnostic accuracy and prognostic significance of blood fibrosis tests and liver stiffness measurement by FibroScan in non-alcoholic fatty liver disease. *J Hepatol* 2016;65:570–578.
- [40] Zimmermann E, Anty R, Tordjman J, Verrijken A, Gual P, Tran A, et al. C-reactive protein levels in relation to various features of non-alcoholic fatty liver disease among obese patients. *J Hepatol* 2011;55:660–665.